Advances in Aircraft and Spacecraft Science, *Vol. 12, No. 3 (2025) 245-267*
https://doi.org/10.12989/aas.2025.12.3.245

Parametric resonance of graphene platelet-reinforced metal foam beams under external excitation and boundary constraints

W.B. Shan*[1,2], H. Li[1], Q.M. Peng[1] and N.N. Zhang[2]

[1]*Hunan Electrical College of Technology, Xiangtan, 411101, PR China*
[2]*Changsha Environmental Protection College, Changsha, 410004, PR China*

(Received July 18, 2024, Revised August 22, 2025, Accepted August 25, 2025)

Abstract. This paper investigates the parametric resonance of graphene-platelet reinforced metal foam (GPLRMF) beams under three typical boundary conditions. The Halpin-Tsai model and rule of mixture are employed to characterize the GPLRMF material properties, while the governing equations are established based on Euler-Bernoulli beam theory. Numerical results demonstrate that increased external excitation leads to significant amplification of vibration amplitudes. The modified variable amplitude method is adopted to ensure accurate prediction of system response across the entire frequency range, with validation against existing literature. Detailed parametric studies examine the effects of: (1) foam distributions (including Foam-I pattern), (2) porosity coefficients, (3) GPL dispersion patterns (Type-A to Type-X), and (4) GPL weight fractions. Furthermore, the influences of boundary constraints, thermal environments, external stimuli, and damping ratios on parametric resonance are systematically analyzed. Key findings indicate that Foam-I distribution with Type-A GPL arrangement exhibits negligible dynamic response, suggesting superior anti-vibration capacity. Both clamped boundaries and reduced temperature are shown to effectively shift resonance positions while enhancing beam stiffness.

Keywords: beams; boundary conditions; GPLRMF; parametric resonance; thermal environment

1. Introduction

Beam structure is the most basic type of structure in engineering, and the study of nonlinear oscillation in beams has been one of the research highlights in recent years (Zhang *et al.* 2022, Hasan and Rahman 2022, Yang *et al.* 2021). This research has immediate significance for numerous fields such as ocean engineering, civil engineering, and aerospace engineering (Khouddar *et al.* 2021). As a basic structure, the beam is important as a reference for the study of plate structures. Furthermore, a beam can be modeled as a solidified model representative of pipelines, making it valuable for exploring pipeline dynamics (Ashraf *et al.* 2022, Chai *et al.* 2020, Shao and Ding 2023, Zhu *et al.* 2020). Consequently, research on nonlinear vibration in beams has attracted widespread interest over time. For instance: Zhao *et al.* (2023) employed the Galerkin truncation method to study the nonlinear dynamic response of foundation beams, considering the effects of excitation methods and parameters. Alimoradzadeh and Akbas (2023) focused on the

*Corresponding author, Professor, E-mail: shanwubin2020@163.com

http://www.techno-press.org/?journal=aas&subpage=7 ISSN: 2287-528X (Print), 2287-5271 (Online)

nonlinear vibration behaviors of beams on elastic foundations using the Euler-Bernoulli beam theory. Using Hamilton's principle, Chen *et al.* (2020) constructed a new beam model based on Hooke's law to investigate its nonlinear free oscillation behavior. Considering geometric nonlinearity among other factors, Zhou *et al.* (2021) examined the nonlinear forced oscillation behaviors of cantilever beams under evenly-distributed loads. Le *et al.* (2023) discussed the influence of homogenization schemes and foundation shoring on the nonlinear oscillation of a sandwich beam using the third-order shear deformation theory. Based on a modified third-order shear deformation theory, Xie *et al.* (2020) proposed an innovative method to address the nonlinear oscillation of functionally graded (FG) beams under moving loads. Wang *et al.* (2021) established models using Rayleigh beam theory to address the free vibration of beams in a humid and hot environment. Rincon-Casado *et al.* (2021) investigated the free nonlinear oscillation frequencies of beams under seven boundary conditions using nonlinear normal modes. Recent studies have systematically investigated the dynamic behaviors of advanced structural systems through various analytical approaches. Wang and colleagues (2025) employed the Rayleigh-Ritz technique to examine mode transition phenomena and natural frequency loci veering in 3D Kagome truss-core sandwich panels. In their earlier work (Wang *et al.* 2019a), the research team applied Extended Melnikov's method to analyze nonlocal nonlinear dynamics, including chaotic and homoclinic behaviors, in forced viscoelastic nanoplates with bilayer configurations. Another significant contribution (Wang *et al.* 2019b) involved comprehensive analytical derivation of frequency-response relationships, bifurcation boundaries, and stability conditions for both subharmonic and ultra-subharmonic responses in an innovative bioinspired nonlinear isolation system. Complementing these findings, Xiong *et al.* (2023) designed a vibration isolation mechanism incorporating biological structural principles and nonlinear absorbers, with particular emphasis on exploring intricate dynamic properties under internal resonance conditions. Mohamed *et al.* (2024) pioneered the derivation of exact analytical solutions and closed-form expressions for nonlinear stability and vibration characteristics in both straight and curved beam systems incorporating viscoelastic boundary conditions. Concurrently, Abouelregal *et al.* (2022) employed Caputo-Fabrizio fractional derivative methodology to investigate thermoelastic wave propagation in nonlocal isotropic solids under pulsed thermal loading, formulating their mathematical model through nonlocal elasticity theory and fractional calculus with single-kernel generalized thermoelasticity. Akbas *et al.* (2022) contributed to micromechanical analysis by developing a dynamic model for simply supported porous functionally graded microbeams under moving loads. Alibakhshi *et al.* (2022) extended this research to dielectric elastomer microbeam resonators, analyzing their nonlinear size-dependent vibrations using a hyperelastic Cosserat continuum framework. Hosseini *et al.* (2023) further expanded the scope by examining depth-dependent in-plane free vibrations in curved functionally graded nanobeams through nonlocal elasticity theory, demonstrating the influence of geometric parameters at nanoscale dimensions. Abouelregal *et al.* (2018) examined the vibrational characteristics of doubly-clamped microbeams under external transverse excitations, employing both the modified couple stress (MCS) theory and a thermoelastic model incorporating Lord-Shulman's heat conduction formulation. Building upon this foundation, Abouelregal *et al.* (2021) investigated thermoelastic vibrations in viscoelastic microbeams supported by Winkler foundations, utilizing fractional-order theory combined with Kelvin-Voigt constitutive relationships. More recently, Alhassan and Abouelregal (2025) developed an innovative analytical framework for studying axial dynamic responses in rotating thermoelastic nanobeams under moving loads. This work represents a significant advancement through the integration of Klein-Gordon nonlocal theory with a novel internal time scale parameter

formulation.

Parametric vibration is a distinct form of vibration caused by periodic variations in system parameters (Mbong *et al.* 2018, Sahoo 2022). The oscillation resulting from periodically changing system parameters is called parametric oscillation. The instability phenomenon occurring in a vibrating mechanical system under cyclical parameter variations is known as parametric resonance (Sahoo *et al.* 2017, Zhu *et al.* 2018, Sahoo and Chatterjee 2021). Currently, nonlinear parametric vibration has garnered extensive attention, and many scholars have conducted profound research on it. For example: Sahoo (2020) used the multi-scale method and a continuous algorithm to study lateral vibration of beams under combined parametric excitation, which arose from the time dependence of axial speed and axial tensile force. Garg and Dwivedy (2020) investigated combined parametric resonance in piezoelectric beams using a generalized Galerkin approach considering two modes, supplemented by relevant resonance experiments for comparative analysis. Considering axial coupling motion, Arvin *et al.* (2020) employed the multi-scale method to examine primary parametric resonance in rotating beams, successfully analyzing the parametric resonance induced by angular velocity. Accounting for the effect of magnetic field steady loadings, Hu *et al.* (2018) analyzed the primary parametric resonance and stability of beams using the multi-scale method. Based on Hamilton's principle, Sheng and Wang (2018) focused on primary resonance and parametric vibration in FG beams. Incorporating the influence of a magnetic field, Li *et al.* (2017) examined nonlinear resonance behavior and stability of circular plates under parametric excitation using Hamilton's principle and the Galerkin method. According to the von Kármán plate theory, Li *et al.* (2020) examined nonlinear vibration of plates considering fluid-structure interaction, obtaining system states that varied continuously with parameter changes. Wang *et al.* (2019) investigated nonlinear dynamics of stiffened plates using thin plate theory and parametric analysis, solving the 3:1 internal resonance problem of the system. Considering the effect of alternating loadings, Hu *et al.* (2018) studied nonlinear combination resonance in circular plates under two excitation types: parametric excitation and transverse excitation. Hamed and Alkhathami (2021) applied multiscale perturbation to investigate nonlinear vibration of plate-cavity systems under parametric excitation, analyzing resonance problems through numerical methods. Under conditions of parametric resonance and 1:3 autoparametric resonance, Zhang *et al.* (2018) studied nonlinear vibration and chaotic motion of rectangular plates under dual incentives. Li (2021) studied nonlinear parametric resonance in cylindrical shells under the effect of initial circumferential tension using nonlinear shell theory. Foroutan and Ahmadi (2022) utilized a semi-analytical approach to study nonlinear vibration in geometrically imperfect cylindrical shells under both axial parametric excitation and external excitation. Based on Reddy's third-order shear deformation theory, Liu *et al.* (2017) explored nonlinear vibration behavior of composite cylindrical shells accounting for parametric excitation due to temperature changes. Under the combined action of parametric resonance and internal resonance, Jahangiri *et al.* (2022) analyzed nonlinear and chaotic behavior of FG hyperbolic shells, investigating conditions leading to different periodic regimes and chaotic phenomena. Gu *et al.* (2021) focused on primary resonance and nonlinear vibration behavior of composite material blades under multiple combined parametric incentives. Carboni *et al.* (2022) employed the multi-scale method to study parametric resonance in piezoelectric beams driven by ripple voltage. Aghamohammadi *et al.* (2023) explored the response of cantilever beams under parametric excitation using the variational amplitude method and multi-scale method.

Graphene platelet reinforced metal foam (GPRMF) beams have demonstrated significant potential in aerospace thermal protection systems and energy-absorbing structures, owing to their

superior strength-to-weight ratio and thermal stability (She *et al*. 2025, Xu *et al*. 2025). Xu *et al*. (2021) presented an investigation on the free vibration behaviors of FG-GPLRMF beams using the differential transformation method. Employing von Kármán's nonlinear plate theory, Teng and Wang (2021) introduced stress functions to explore the nonlinear forced oscillation phenomenon of GPLRMF plates. Yang *et al*. (2022) dealt with the impulse response of GPLRMF plates, in which the influence of foam distributed modes and other factors on the impact response was analyzed. Wang *et al*. (2019) focused on the nonlinear oscillation behaviors of GPLRMF cylindrical shells using a modified Donnell nonlinear shell theory to establish their model. Mirjavadi *et al*. (2019) explored the forced oscillation behaviors of GPL composite shells with pores using first-order shell theory and semi-analytical methods. Considering the effect of external loads, Al-Furjan *et al*. (2021) mathematically derived the nonlinear frequency of GPL-reinforced hyperbolic panels using the generalized differential quadrature approach.

Although numerous studies have been conducted on the nonlinear oscillations of beams, a literature review reveals that there is still a gap in the research on the parametric resonance of GPLRMF beams under different boundary conditions. Therefore, to fill this gap, this article investigates parametric resonance in GPLRMF beams under three different boundary conditions.

2. Construction of control equations

Fig. 1 presents a schematic diagram of the GPLRMF beams within the coordinate system. This study investigates three distinct foam distribution patterns: Foam-I (uniform), Foam-II (gradient), and Foam-III (hybrid). The composite material comprises two primary components: graphene platelets (GPL) as reinforcement and metal foam as the matrix. Following Fan *et al*. (2025) classification, the GPL reinforcement is distributed in three configurations: randomly oriented, functionally graded, and aligned patterns. To determine the effective material properties, we employ a combined approach utilizing the rule of mixtures for preliminary estimates and the Halpin-Tsai micromechanical model for more accurate predictions of stiffness enhancement. This methodology enables comprehensive characterization of the mechanical properties while accounting for the complex interactions between the GPL reinforcement and porous metal matrix (Cheng and She 2025a, 2025b, Cheng *et al*. 2025).

$$
\begin{aligned}
E(z) &= \begin{cases} E^{\#}\left[1-e_1\cos\Upsilon\right], & \text{(Foam-I)} \\ E^{\#}\left\{1-e_2\left[1-\cos\Upsilon\right]\right\}, & \text{(Foam-II)} \\ E^{\#}e_3, & \text{(Foam-III)} \end{cases} \\
\alpha(z) &= \begin{cases} \alpha^{\#}\left[1-e_1\cos\Upsilon\right], & \text{(Foam-I)} \\ \alpha^{\#}\left\{1-e_2\left[1-\cos\Upsilon\right]\right\}, & \text{(Foam-II)} \\ \alpha^{\#}e_3, & \text{(Foam-III)} \end{cases} \\
\rho(z) &= \begin{cases} \rho^{\#}\left[1-e_{m1}\cos\Upsilon\right], & \text{(Foam-I)} \\ \rho^{\#}\left\{1-e_{m2}\left[1-\cos\Upsilon\right]\right\}, & \text{(Foam-II)} \\ \rho^{\#}e_{m3}, & \text{(Foam-III)} \end{cases} \\
\mu(z) &= \mu^{\#}
\end{aligned}
\tag{1}
$$

Where $\gamma=\pi z/h$ represents the dimensionless coordinate through the beam thickness. For solid

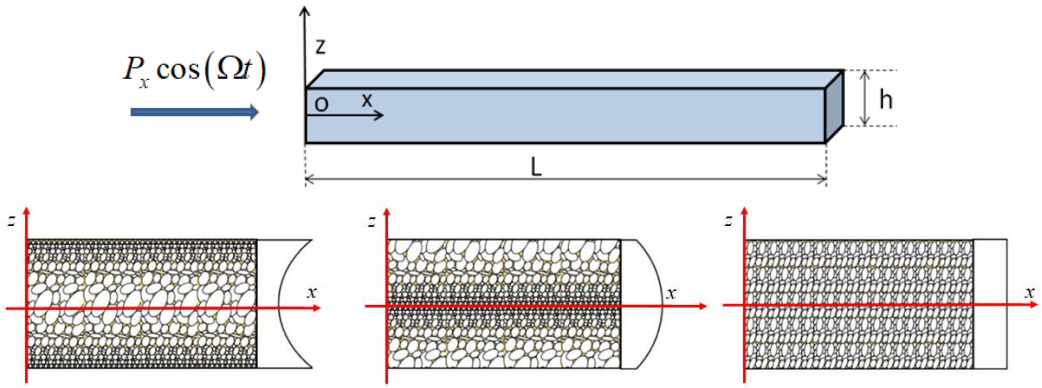

Fig. 1 Structural schematic diagram of the GPLRMF beam (Modified from Ma *et al.* 2025)

beams (without pores), the material parameters are defined as: Young's modulus ($E^{\#}$), thermal expansion coefficient ($\alpha^{\#}$), Poisson's ratio ($\mu^{\#}$), and mass density ($\rho^{\#}$). These baseline properties serve as reference values for subsequent porous beam analyses (Wang *et al.* 2019, Zhao and She 2025).

$$\begin{aligned} E^{\#} &= \frac{3}{8}\left(\frac{1+\zeta_L\eta_L V_{gpl}}{1-\eta_L V_{gpl}}\right)E_m + \frac{5}{8}\left(\frac{1+\zeta_W\eta_W V_{gpl}}{1-\eta_W V_{gpl}}\right)E_m \\ \alpha^{\#} &= \alpha_{gpl}V_{gpl} + \alpha_m\left(1-V_{gpl}\right) \\ \mu^{\#} &= \mu_{gpl}V_{gpl} + \mu_m\left(1-V_{gpl}\right) \\ \rho^{\#} &= \rho_{gpl}V_{gpl} + \rho_m\left(1-V_{gpl}\right) \end{aligned} \tag{2}$$

in which

$$\begin{aligned} \zeta_L &= \frac{2l_{gpl}}{t_{gpl}}, \zeta_W = \frac{2w_{gpl}}{t_{gpl}} \\ \eta_L &= \frac{E_{gpl}-E_m}{E_{gpl}+\zeta_L E_m}, \eta_W = \frac{E_{gpl}-E_m}{E_{gpl}+\zeta_W E_m} \end{aligned} \tag{3}$$

In equations related to material physical parameters, In the constitutive equations describing material properties, the subscripts "*gpl*" and "*m*" denote the physical parameters of graphene platelets (GPL) and metal matrix respectively, including elastic modulus, density, and thermal properties. Furthermore, the material's mechanical performance exhibits significant temperature dependence, as both constituent materials demonstrate distinct thermomechanical behaviors that collectively influence the composite's overall response under varying thermal conditions.

$$\Gamma_i = \Gamma_0\left(\frac{\Gamma_{-1}}{T}+1+\Gamma_1 T+\Gamma_2 T^2+\Gamma_3 T^3\right), \quad (i=gpl,m) \tag{4}$$

In the constitutive equations, Γ represents the material parameter set (E, α, μ, ρ), where Γ_1 to Γ_3 denote temperature-dependent coefficients. Three GPL distribution patterns are investigated: GPL-

A (uniform), GPL-B (gradient), and GPL-C (random), and (Li and She 2025)

$$V_{gpl}=\begin{cases}S_{i1}\left[1-\cos\Upsilon\right], & \text{(GPL-A)}\\ S_{i2}\cos\Upsilon, & \text{(GPL-B)}\\ S_{i3}, & \text{(GPL-C)}\end{cases} \tag{5}$$

in which

$$\frac{E(z)}{E^{*}}=\left[\frac{\rho(z)}{\rho^{*}}\right]^{2} \tag{6}$$

By substituting Eq. (2) into Eq. (6), we obtain the following relationship (Ma *et al.* 2025)

$$\begin{cases}1-e_{m1}\cos\Upsilon=\sqrt{1-e_1\cos\Upsilon}\\ 1-e_{m2}\left[1-\cos\Upsilon\right]=\sqrt{1-e_2\left[1-\cos\Upsilon\right]}\\ e_{m3}=\sqrt{e_3}\end{cases} \tag{7}$$

in which

$$\int_0^{\frac{h}{2}}\sqrt{1-e_1\cos\Upsilon}dz=\int_0^{\frac{h}{2}}\sqrt{1-e_2\left[1-\cos\Upsilon\right]}dz=\int_0^{\frac{h}{2}}\sqrt{e_3}dz \tag{8}$$

Based on Euler-Bernoulli beam theory, the displacement field of the beam can be expressed in the following form (Abouelregal *et al.* 2020, 2022, 2024)

$$\begin{aligned}u_1(x,z,t)&=u(x,t)-z\frac{\partial w(x,t)}{\partial x}\\ u_2(x,z,t)&=0\\ u_3(x,z,t)&=w(x,t)\end{aligned} \tag{9}$$

In the expressions of displacement field, t expresses time and u represents the axial displacement of the model. It should be noted that during the research process, the Euler-Bernoulli beam theory employed in this parametric resonance analysis exhibits certain limitations: (a) Neglect of shear effects: The model assumes negligible shear deformation, which becomes problematic for beams with low shear modulus or significant thickness, where shear effects substantially influence resonance behavior. (b) Simplified cross-section assumptions: The theory enforces rigid cross-section behavior (excluding warping), thereby limiting its accuracy in analyzing parametric resonance of complex geometries undergoing torsional-axial coupling. (c) Frequency range constraints: The theory's accuracy diminishes when studying super-harmonic/subharmonic resonances due to its inability to properly model higher-order wave interactions. (d) For studies involving complex boundary conditions, more sophisticated models such as Timoshenko beam theory or higher-order theories are typically necessary (Abouelregal and Tiwari 2022).

Taking the displacement strain relationship into account, the nonlinear strain of GPLRMF beam has the following general form

$$\varepsilon_{xx}=\frac{\partial u_1}{\partial x}+\frac{1}{2}\left(\frac{\partial u_3}{\partial x}\right)^{2}=\frac{\partial u}{\partial x}+\frac{1}{2}\left(\frac{\partial w}{\partial x}\right)^{2}-z\frac{\partial^{2}w}{\partial x^{2}} \tag{10}$$

When regarding the effect of temperature field, in order to simplify the research calculation, this paper takes the case of a well-distributed temperature field. Then calculation of σ_{xx} can be carried out according to the following equation.

$$\sigma_{xx} = E(z)\left[\varepsilon_{xx} - \alpha(z)\Delta T\right] \tag{11}$$

In the above equation, ΔT represents the part where the temperature rises, and its corresponding relation with the ambient temperature T is: $\Delta T=T$-300 K. In numerous practical uses, it includes many temperature fields, and our research puts to use the uniform temperature field that is simple for calculation (Zhang *et al*. 2023).

Subsequently, the internal torque has the following expression forms.

$$\begin{aligned} N_x &= A_1\left(\frac{\partial u}{\partial x} + \frac{1}{2}\left(\frac{\partial w}{\partial x}\right)^2\right) - B_1\frac{\partial^2 w}{\partial x^2} - N_T \\ M_x &= B_1\left(\frac{\partial u}{\partial x} + \frac{1}{2}\left(\frac{\partial w}{\partial x}\right)^2\right) - D_1\frac{\partial^2 w}{\partial x^2} \end{aligned} \tag{12}$$

N_T represents the thermal related loading, A_1, B_1, D_1 stand for stiffness, and their calculation formulas are (Zhang *et al*. 2023)

$$\begin{aligned} &\{A_1, B_1, D_1\} = \int_{-h/2}^{h/2} E(z)\{1, z, z^2\}\,\mathrm{d}z, \\ &N_T = \int_{-h/2}^{h/2} \alpha\Delta T E(z)dz = \alpha_1\Delta T, \\ &\alpha_1 = \int_{-h/2}^{h/2} \alpha E(z)dz \end{aligned} \tag{13}$$

Next, δU represents strain energy.

$$\begin{aligned} \delta U &= \delta\int_{t_1}^{t_2}\left(\frac{1}{2}\int_0^L\int_{-\frac{h}{2}}^{\frac{h}{2}}\sigma_x\varepsilon_x dxdz\right)dt \\ &= \int_{t_1}^{t_2}\int_0^L\int_{-\frac{h}{2}}^{\frac{h}{2}}\sigma_x\delta\varepsilon_x dxdzdt \\ &= \int_{t_1}^{t_2}\int_0^L\left(N_x\delta\left(\frac{\partial u}{\partial x} + \frac{1}{2}\left(\frac{\partial w}{\partial x}\right)^2\right) - M_x\delta\frac{\partial^2 w}{\partial x^2}\right)dxdt \\ &= \int_{t_1}^{t_2}\int_0^L\left(\left\{-\frac{\partial N_x}{\partial x}\right\}\delta u + \left\{-N_x\frac{\partial^2 w}{\partial x^2} - \frac{d^2 M_x}{dx^2}\right\}\delta w\right)dxdt \end{aligned} \tag{14}$$

The kinetic energy δT is

$$\begin{aligned} \delta T &= \delta\int_{t_1}^{t_2}\left(\frac{1}{2}\int_0^L\int_{-\frac{h}{2}}^{\frac{h}{2}}\rho\left(\dot{u}_1^2 + \dot{u}_2^2 + \dot{u}_3^2\right)dxdz\right)dt \\ &= \int_{t_1}^{t_2}\int_0^L\int_{-\frac{h}{2}}^{\frac{h}{2}}\rho\left[\left(\dot{u} - z\frac{\partial\dot{w}}{\partial x}\right)\delta\left(\dot{u} - z\frac{\partial\dot{w}}{\partial x}\right) + \dot{w}\delta\dot{w}\right]dxdzdt \\ &= \int_{t_1}^{t_2}\int_0^L\begin{bmatrix} -\left(I_0\ddot{u} - I_1\dfrac{\partial\ddot{w}}{\partial x}\right)\delta u - \\ \left(I_0\ddot{w} + I_1\dfrac{\partial\ddot{u}}{\partial x} + I_2\dfrac{\partial^2\ddot{w}}{\partial x^2}\right)\delta w \end{bmatrix}dxdt \end{aligned} \tag{15}$$

where $I_i = \int_{-\frac{h}{2}}^{\frac{h}{2}} \rho z^i \, dz, (i = 0,1,2)$

The work done by external force δW is

$$\delta W = \int_{t_1}^{t_2} \left(-\int_0^L F_x w \delta w dx - \int_0^L C_t \frac{\partial \dot{w}}{\partial x} \delta w dx \right) dt \tag{16}$$

The Hamilton's principle is

$$\delta \int_{t_1}^{t_2} (T - U + W) dt = 0 \tag{17}$$

Through variational processing, it can be obtained that

$$\begin{aligned} &\frac{\partial N_x}{\partial x} = I_0 \ddot{u} - I_1 \frac{\partial \ddot{w}}{\partial x} \\ &N_x \frac{\partial^2 w}{\partial x^2} + \frac{\partial^2 M_x}{\partial x^2} + F_x w - C_t \frac{\partial \dot{w}}{\partial t} = I_0 \ddot{w} + I_1 \frac{\partial \ddot{u}}{\partial x} + I_2 \frac{\partial^2 \ddot{w}}{\partial x^2} \end{aligned} \tag{18}$$

Substitute Eq. (12) into Eq. (18), which can be written as

$$\frac{\partial}{\partial x} \left(A_1 \left(\frac{\partial u}{\partial x} + \frac{1}{2} \left(\frac{\partial w}{\partial x} \right)^2 \right) - B_1 \frac{\partial^2 w}{\partial x^2} - N_T \right) = I_0 \ddot{u} - I_1 \frac{\partial \ddot{w}}{\partial x} \tag{19}$$

$$\begin{aligned} &\left(A_1 \left(\frac{\partial u}{\partial x} + \frac{1}{2} \left(\frac{\partial w}{\partial x} \right)^2 \right) - B_1 \frac{\partial^2 w}{\partial x^2} - N_T \right) \frac{\partial^2 w}{\partial x^2} \\ &+ \frac{\partial^2}{\partial x^2} \left(B_1 \left(\frac{\partial u}{\partial x} + \frac{1}{2} \left(\frac{\partial w}{\partial x} \right)^2 \right) - D_1 \frac{\partial^2 w(x)}{\partial x^2} \right) \\ &+ F_x w - C_t \frac{\partial \dot{w}}{\partial t} = I_0 \ddot{w} + I_1 \frac{\partial \ddot{u}}{\partial x} + I_2 \frac{\partial^2 \ddot{w}}{\partial x^2} \end{aligned} \tag{20}$$

Then, by integrating Eq. (19), both sides of the equation can be transformed into the following form

$$u = -\int_0^x \frac{1}{2} \left(\frac{\partial w}{\partial x} \right)^2 dx + \frac{B_1}{A_1} \frac{\partial w}{\partial x} + b_1 x + b_2 \tag{21}$$

By making $u(0)=u(L)=0$, we can obtain

$$b_1 = \int_0^L \frac{1}{2L} \left(\frac{\partial w}{\partial x} \right)^2 dx, b_2 = 0 \tag{22}$$

By substituting Eqs. (21)-(22) into Eqs. (19)-(20), we can get hold of the following expression.

$$\begin{aligned} &\left(A_1 \int_0^L \frac{1}{2L} \left(\frac{\partial w}{\partial x} \right)^2 dx - N_T \right) \frac{\partial^2 w}{\partial x^2} + \left(\frac{B_1^2}{A_1} - D_1 \right) \frac{\partial^4 w}{\partial x^4} \\ &+ F_x w - C_t \frac{\partial \dot{w}}{\partial t} = I_0 \ddot{w} + I_2 \frac{\partial^2 \ddot{w}}{\partial x^2} \end{aligned} \tag{23}$$

It should be emphasized that in this study, the assumptions of a uniform temperature field and linear damping simplify the analytical process, but they may overlook higher-order resonance modes and amplitude abrupt changes caused by temperature non-uniformity and damping nonlinearity in actual systems. Such assumptions are suitable for preliminary analysis.

To ensure the correctness of the solution, the MVA method is employed (Aghamohammadi *et al.* 2019, Cheng and She 2025b). In the process of seeking answers, three boundary conditions for GPLRMF beam structure are considered, namely simply supported (S-S), fixed supported (C-C), and combination of simply supported and fixed supported (C-S). The solutions under different boundary conditions can be written in the following form (Aghamohammadi *et al.* 2019).

For S-S

$$\begin{aligned} w &= W\sin(\frac{\pi x}{L}), \\ \phi &= \Phi\cos(\frac{\pi x}{L}), \end{aligned} \tag{24}$$

For C-C

$$\begin{aligned} w &= W\left(1-\cos(2\frac{\pi x}{L})\right), \\ \phi &= \Phi\sin(2\frac{\pi x}{L}), \end{aligned} \tag{25}$$

For C-S

$$\begin{aligned} w &= W\left(\cos\left(\frac{\pi x}{2L}\right)-\cos(\frac{3\pi x}{2L})\right), \\ \phi &= \Phi\left(\sin\left(\frac{\pi x}{2L}\right)-3\sin(\frac{3\pi x}{2L})\right), \end{aligned} \tag{26}$$

We apply the MVA method for solving.

$$I\ddot{W}+F_0\dot{W}+F_1W+F_3W^3=WP_x\cos(\Omega t) \tag{27}$$

For S-S

$$\begin{aligned} I &= \frac{I_0L^2-I_2\pi^2}{2L} \\ F_0 &= \frac{C_tL}{2} \\ F_1 &= \frac{D_1\pi^4}{2L^3}-\frac{N_T\pi^2}{2L}-\frac{B_1^2\pi^4}{2A_1L^3} \\ F_3 &= \frac{A_1\pi^4}{8L^3}-\frac{N_T\pi^2}{L}+\frac{D_1\pi^4}{L^3}-\frac{B_1^2\pi^4}{A_1L^3} \\ P_x &= \frac{F_xL}{2} \end{aligned} \tag{28}$$

For C-C

$$
\begin{aligned}
I &= \frac{3I_0L^2 - 4I_2\pi^2}{2L} \\
F_0 &= \frac{3C_tL}{2} \\
F_1 &= \frac{8D_1\pi^4}{L^3} - \frac{2N_T\pi^2}{L} - \frac{8B_1^2\pi^4}{A_1L^3} \\
F_3 &= \frac{2A_1\pi^4}{L^3} - \frac{4N_T\pi^2}{L} + \frac{16D_1\pi^4}{L^3} - \frac{16B_1^2\pi^4}{A_1L^3} \\
P_x &= \frac{3F_xL}{2}
\end{aligned}
\tag{29}
$$

For C-S

$$
\begin{aligned}
I &= \frac{4I_0L^2 - 5I_2\pi^2}{4L} \\
F_0 &= C_tL \\
F_1 &= \frac{41D_1\pi^4}{16L^3} - \frac{5N_T\pi^2}{4L} - \frac{41B_1^2\pi^4}{16A_1L^3} \\
F_3 &= \frac{25A_1\pi^4}{32L^3} - \frac{5N_T\pi^2}{2L} + \frac{41D_1\pi^4}{8L^3} - \frac{41B_1^2\pi^4}{8A_1L^3} \\
P_x &= F_xL
\end{aligned}
\tag{30}
$$

in which (Aghamohammadi *et al.* 2019),

$$\ddot{W} + f_0\dot{W} + \omega_n^2\left(1 - P\cos(\Omega t)\right)W + f_3W^3 = 0 \tag{31}$$

In the above equation,

$$f_0 = F_0/I, \omega_n^2 = F_1/I, P = P_x/F_1, f_3 = F_3/I. \tag{32}$$

Using the MVA approach, let its solution be

$$W = A(t)\cos\left(\frac{1}{2}\Omega t\right) + B(t)\sin\left(\frac{1}{2}\Omega t\right) \tag{33}$$

Substituting the solution into Eq. (23), we can receive (Cheng and She 2025b),

$$
\begin{aligned}
&\ddot{A} + \Omega\dot{B} + f_0\dot{A} + \frac{1}{2}f_0\Omega B - \frac{1}{4}\Omega^2A + \\
&\omega_L^2A\left(1 + \frac{1}{2}P\right) + \frac{3}{4}f_3A\left(A^2 + B^2\right) = 0
\end{aligned}
\tag{34}
$$

$$
\begin{aligned}
&\left(\begin{aligned}
&\ddot{B} - \Omega\dot{A} + f_0\dot{B} - \frac{1}{2}f_0\Omega A - \frac{1}{4}\Omega^2B \\
&+\omega_n^2B\left(1 - \frac{1}{2}P\right) + \frac{3}{4}f_3B\left(A^2 + B^2\right)
\end{aligned}\right)\sin\left(\frac{1}{2}\Omega t\right) = \\
&-\left(\frac{1}{2}PA\omega_n^2 + \frac{1}{4}f_3A\left(A^2 - 3B^2\right)\right)\cos\left(\frac{3}{2}\Omega t\right)
\end{aligned}
$$

$$-\left(\frac{1}{2}PB\omega_n^2+\frac{1}{4}f_3B\left(3A^2-B^2\right)\right)\sin\left(\frac{3}{2}\Omega t\right) \tag{35}$$

In an effort to achieve the steady-state approximate solution of the equation, the derivative terms for time t in the above equation are all 0. After that

$$\frac{1}{2}f_0\Omega B-\frac{1}{4}\Omega^2A+\omega_L^2A\left(1+\frac{1}{2}P\right)+\frac{3}{4}f_3A\left(A^2+B^2\right)=0 \tag{36}$$

$$-\frac{1}{2}f_0\Omega A-\frac{1}{4}\Omega^2B+\omega_n^2B\left(1-\frac{1}{2}P\right)+\frac{3}{4}f_3B\left(A^2+B^2\right)=0 \tag{37}$$

Based on MVA, the amplitude frequency relationship of the solution can be written as

$$D^2=\frac{1}{3f_3}\left(\Omega^2-4\omega_n^2\pm2\sqrt{\left(\omega_n^2P\right)^2-\left(f_1\Omega\right)^2}\right) \tag{38}$$

3. Discussion of numerical results

This section presents numerical research results on parametric resonance of GPLRMF beams. To validate the methodology, Table 1 compares natural frequency values from existing literature with computational results, demonstrating the approach's reliability through CC and C-S boundary condition comparisons. Table 2 specifies the material parameters used in the analysis. For the magnitude-frequency response curves, the numerical results of the method employed in this paper are compared with those of the fourth-order Runge-Kutta method in Fig. 2. The data show excellent agreement, confirming the validity and correctness of the present work.

Fig. 3 systematically compares three distinct pore distribution patterns (Foam-I, Foam-II,

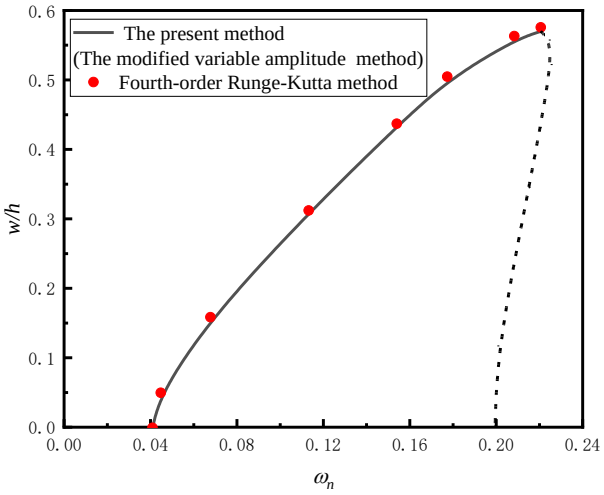

Fig. 2 Comparison of the present method with fourth-order Runge-Kutta results (L=1 m, h=0.03 m, *GPL-B*, T=300 K, W_{gpl}=1%, e_1=0.3, S-S)

Table 1 Comparison of natural frequencies of beams under two boundary conditions

	C-C			C-S		
	ω_1	ω_2	ω_3	ω_1	ω_2	ω_3
Present	5.58	15.31	29.85	2.45	9.78	21.30
Li *et al.* (2019)	5.56	15.09	28.89	2.45	9.69	21.32
Yang and Chen (2008)	5.59	15.42	30.23	2.47	9.87	22.21

Table 2 Physical parameters of relevant materials (Wang and Zhang 2022)

Materials	Properties	Γ_{-1}	Γ_0	Γ_1	Γ_2	Γ_3
Nickel	E_m (Pa)	0	223.95×10^{9}	-2.974×10^{-4}	-3.998×10^{-9}	0
	μ_m	0	0.31	0	0	0
	ρ_m (kg/m^3)	0	8908	0	0	0
	α_m (1/K)	0	9.9209×10^{-6}	8.7056×10^{-4}	0	0
GPLs	E_{gpl} (Pa)	0	1087.8×10^{9}	-0.261×10^{9}	0	0
	μ_{gpl}	0	0.186	0	0	0
	ρ_{gpl} (kg/m^3)	0	1060	0	0	0
	α_{gpl} (1/K)	0	13.920×10^{-6}	-0.0299×10^{-6}	0	0

Foam-III) under identical boundary conditions. While the resonance curves exhibit similar qualitative trends, Foam-I demonstrates higher resonance frequencies and lower peak amplitudes compared to Foam-II, which exhibits the lowest natural frequency and maximum dynamic deflection. These variations highlight the critical role of pore architecture in governing nonlinear dynamic behavior, providing valuable insights for optimizing composite structures in vibration-sensitive applications. Also, it can be seen that S-S conditions result in greater radial displacement compared to C-S, while C-C conditions produce minimal deformation due to enhanced structural stiffness, as evidenced by the rightward shift in the resonance curve. These findings underscore the importance of boundary constraints in tailoring the dynamic response of advanced composite materials for specific engineering requirements.

Fig. 4 investigates the influence of GPLs distribution patterns (GPL-A and GPL-B) on the dynamic response of the composite beam. The study demonstrates that GPL-B initiates resonance at lower frequencies compared to GPL-A, indicating a reduced stiffness-to-inertia ratio. Conversely, GPL-A exhibits superior vibration suppression characteristics, as evidenced by its delayed resonance onset and lower dynamic deflection magnitudes. These findings underscore the critical role of GPL distribution in tailoring the mechanical behavior of advanced composite materials, with GPL-A emerging as the more favorable configuration for applications requiring enhanced vibration damping.

Fig. 5 explores temperature effects on GPLRMF beams, revealing a leftward shift in the resonance curve with increasing temperature. This shift corresponds to reduced natural frequencies and increased radial deformation, indicating thermal softening effects that degrade vibration resistance at elevated temperatures. These results emphasize the necessity of thermal management strategies in high-temperature applications, such as aerospace and civil infrastructure, where maintaining structural integrity under varying environmental conditions is paramount.

Fig. 6 analyzes the effect of GPL volume fraction (W_{gpl}) on the amplitude-frequency response

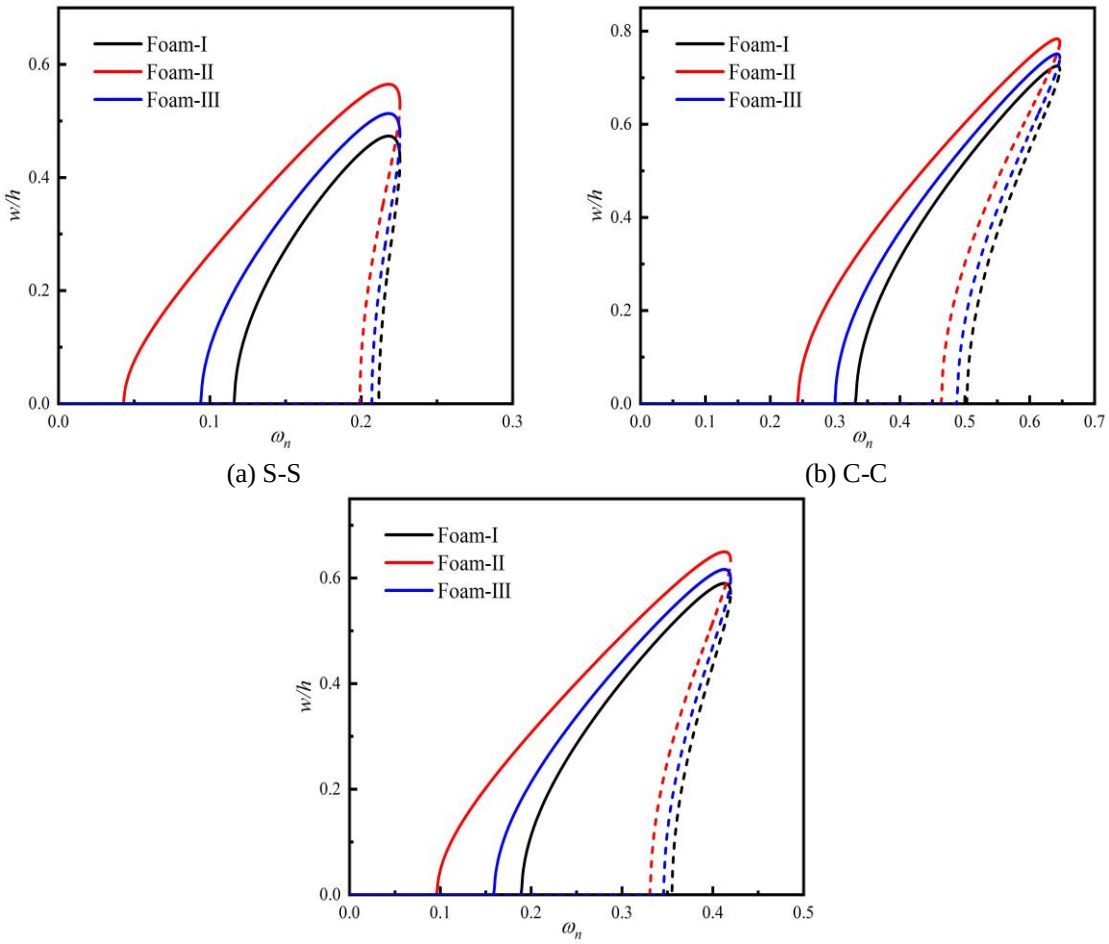

Fig. 3 Influence of foams distribution (L=1 m, h=0.03 m, *GPL-B*, T=300 K, W_{gpl}=1%, e_1=0.3)

of GPLRMF beams under the configuration: Foam-I pore distribution, GPL-B pattern, length L=1 m, thickness h=0.03 m, temperature T=300 K, and porosity coefficient e_1=0.3. For the S-S boundary condition, increasing W_{gpl} from 0.2% to 1.0% reduces the maximum radial deflection by approximately 23%. Similar reductions occur under other boundary conditions, where the peak amplitude of the parametric resonance curve decreases as W_{gpl} rises. Furthermore, higher W_{gpl} values increase the fundamental frequency and shift the resonance position toward higher frequencies, indicating its significant role in modifying the beam's dynamic response.

Fig. 7 analyzes the impact of porosity coefficient (e_1) on the parametric resonance response of GPLRMF beams. The study reveals systematic variations in dynamic behavior, with trends that partially align with those observed for pore distribution types, GPL patterns, volume fractions, and temperature—yet distinct differences emerge. As e_1 increases from 0 to 0.6, dynamic deflection escalates progressively, correlating with heightened resonance curve peaks. However, frequency responses exhibit divergence: solid-line curves indicate higher frequencies at lower e_1 values, whereas dashed curves demonstrate an inverse relationship. This contrast underscores porosity's

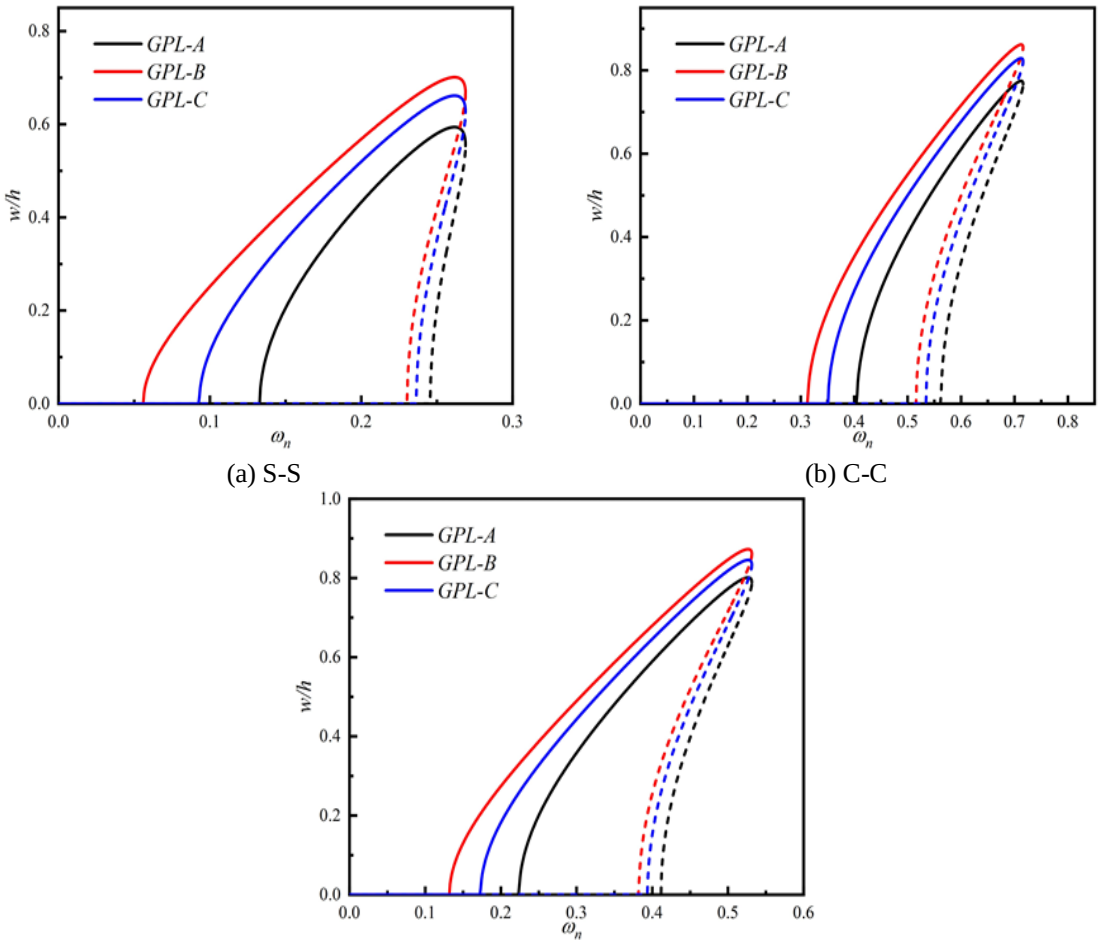

(a) S-S (b) C-C

(c) C-S

Fig. 4 Influence of GPL pattern (L=1 m, h=0.03 m, Foam-I, T=300 K, W_{gpi}=1%, e_1=0.3)

unique influence, differentiating its effects from previously identified patterns.

Fig. 8 investigates the role of external excitation in the dynamic response of GPLRMF beams under transverse loading. Resonance curves for S-S, C-C, and C-S boundaries exhibit consistent trends. External excitation markedly amplifies peak amplitudes in the nonlinear dynamic response and broadens the resonance bandwidth. Critically, the resonance frequency position remains invariant despite variations in excitation intensity. These observations confirm that external excitation primarily enhances radial deflection and dynamic deformation without altering the fundamental resonance frequency locus.

Fig. 9 explores damping effects on resonance behavior. Mirroring the findings for external excitation, damping variations do not shift resonance frequencies but directly influence peak amplitudes. Under S-S, for instance, increasing damping from 5×10^4 to 8×10^4 results in negligible resonance frequency change but reduces radial amplitude by approximately 54%. Concurrently, the resonance bandwidth contracts significantly. This reaffirms damping's primary function in energy dissipation rather than resonance timing modulation.

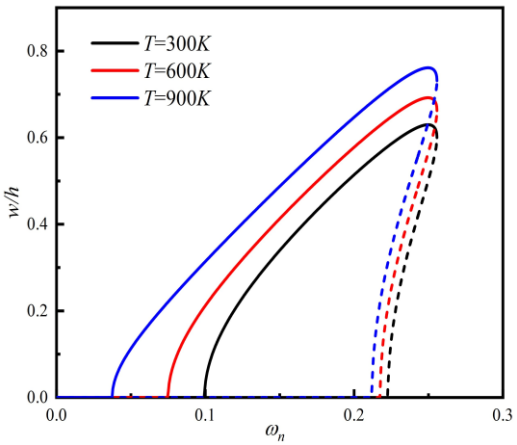

(a) S-S

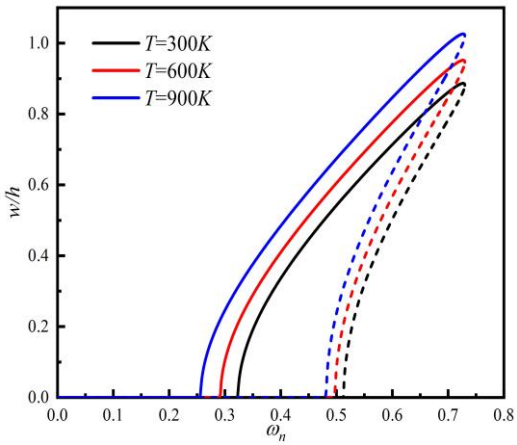

(b) C-C

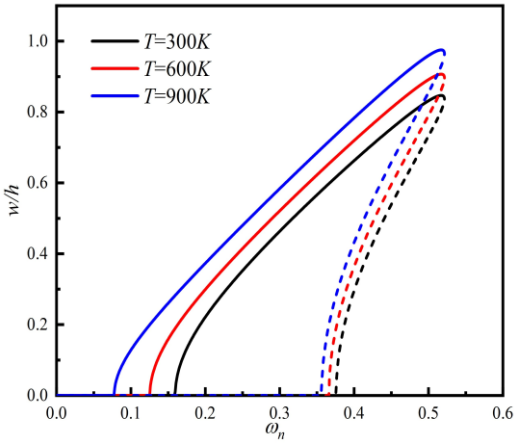

(c) C-S

Fig. 5 Influence of temperature (L=1 m, h=0.03 m, Foam-I, *GPL-B*, W_{gpl}=1%, e_1=0.3)

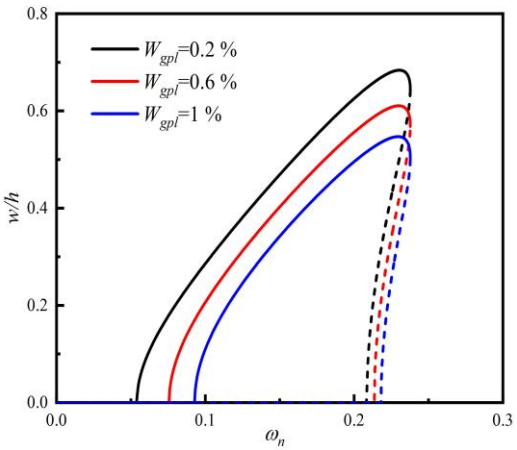

(a) S-S

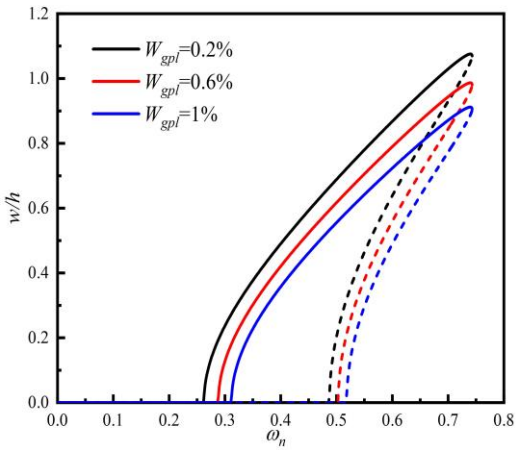

(b) C-C

Fig. 6 Influence of GPL weight fraction (L=1 m, h=0.03 m, Foam-I, *GPL-B*, T=300 K, e_1=0.3)

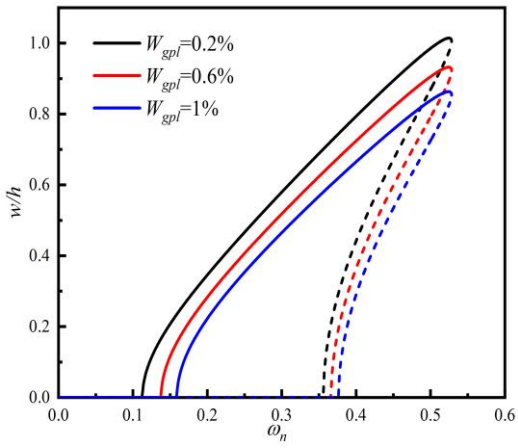

(c) C-S

Fig. 6 Continued

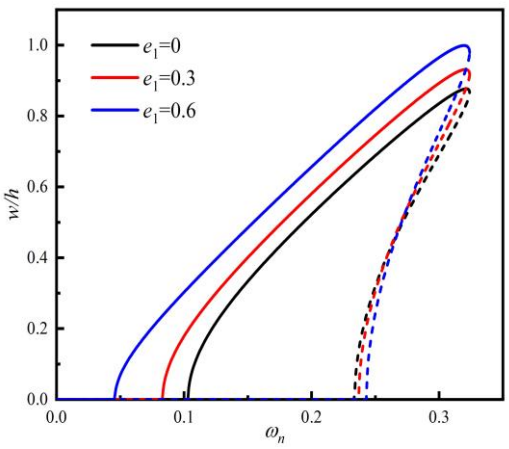

(a) S-S

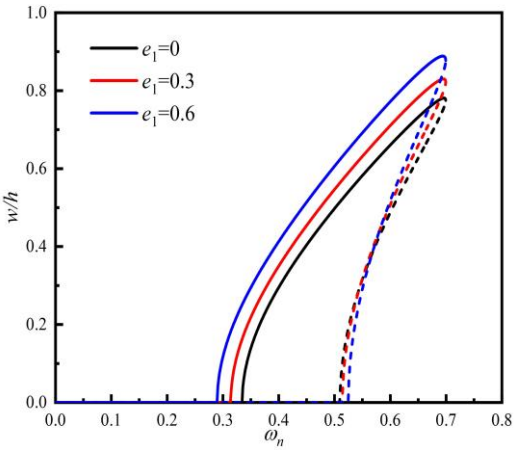

(b) C-C

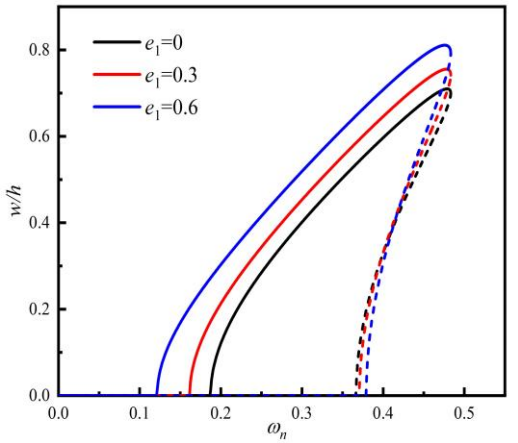

(c) C-S

Fig. 7 Influence of foam coefficient (L=1 m, h=0.03 m, Foam-I, *GPL-B*, T=300 K, W_{gpl}=1%)

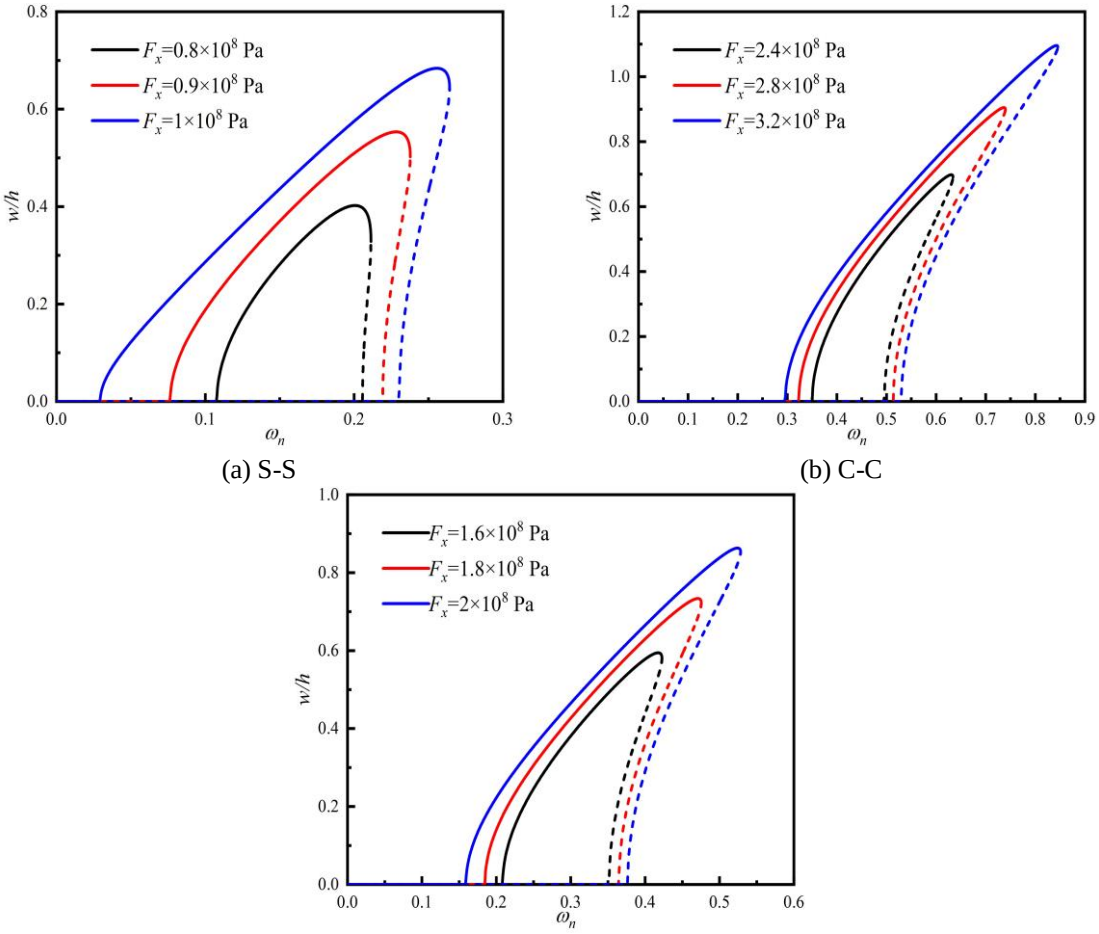

(a) S-S (b) C-C

(c) C-S

Fig. 8 Influence of external excitation (L=1 m, h=0.03 m, Foam-I, *GPL-B*, T=300 K, W_{gpl}=1%, e_1=0.3)

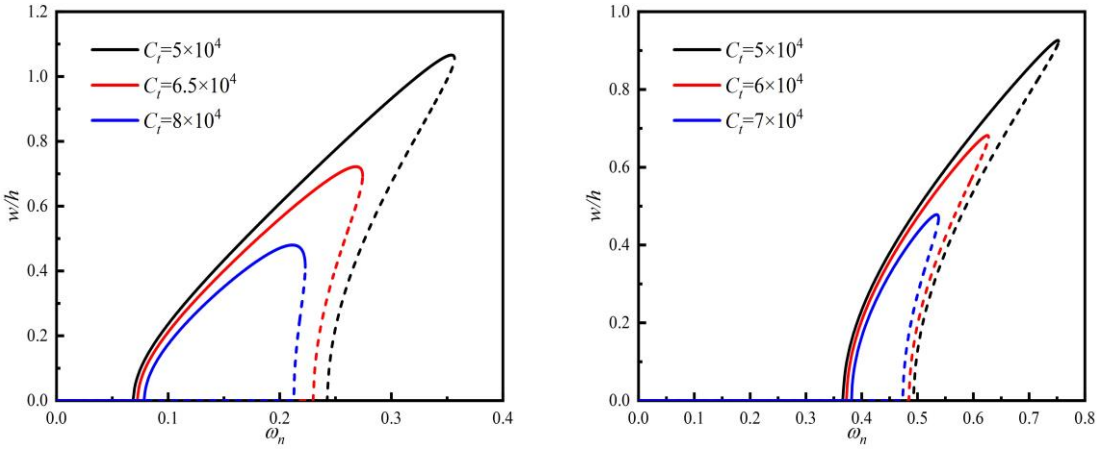

(a) S-S (b) C-C

Fig. 9 Influence of damping (L=1 m, h=0.03 m, Foam-I, *GPL-B*, T=300 K, W_{gpl}=1%, e_1=0.3)

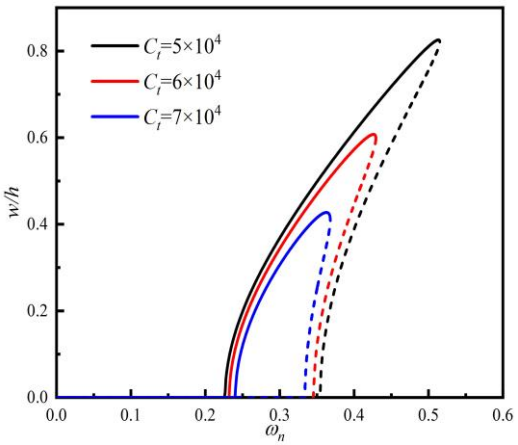

(c) C-S

Fig. 9 Continued

4. Conclusions

This paper presents modeling and research on a nonlinear external excitation system, with particular focus on investigating the effects of various influencing factors on the parametric resonance of GPLRMF beams. The study methodology comprises four key phases: First, material parameters were determined using the mixing law and Halpin-Tsai model. Second, the governing equations were systematically established. Third, the multi-variable analysis approach was implemented to accurately predict the system's response across the entire frequency spectrum. The obtained results were then rigorously validated against existing literature to ensure methodological accuracy. Finally, through comprehensive analysis of nonlinear dynamic responses under varying influencing factors, significant insights were derived regarding the parametric resonance characteristics of GPLRMF beams.

(1) Boundary Conditions: S-S boundary yields maximum dynamic deflection, while C-C exhibits minimum displacement, confirming fixed constraints enhance structural stiffness.

(2) Porosity Effects: Foam-I porosity minimizes radial deformation, whereas Foam-II maximizes it under identical conditions.

(3) GPL Distribution: Resonance occurs earliest in GPL-A mode (vs. GPL-B/C), with higher Wgpl values delaying resonance onset, suggesting GPL-A with elevated W_{gpl} optimizes vibration resistance.

(4) Temperature Sensitivity: Lower temperatures reduce radial amplitude and delay resonance, improving beam stiffness and thermal stability.

(5) Porosity Coefficient (e_1): Smaller e_1 values decrease peak deflection, pre-/post-resonance frequency trends invert with e_1 variation.

(6) External Factors: Excitation force (F) and damping (C_t) alter curve peaks without shifting resonance position—higher F increases deflection, while reduced Ct expands resonance domain.

The findings of this study offer significant implications for engineering applications: (a) Aerospace—lightweighted fuselage components with enhanced vibration resistance, (b) Civil

engineering— energy-absorbing structures for seismic zones, and (c) Vibration suppression — tunable dampers leveraging the correlation between porosity distribution and deflection. This work comprehensively demonstrates how material composition, structural constraints, and environmental conditions fundamentally govern the dynamic behavior of GPLRMF beams. These insights are invaluable for applications requiring vibration control and thermal stability. Our systematic investigation advances the understanding of advanced composite materials under multifunctional operational demands, supporting their optimization for aerospace and civil infrastructure. Future research could explore hybrid pore-GPL distributions or multi-physics coupling effects to further enhance performance.

Acknowledgement

We gratefully acknowledge the financial support from the following funding projects: Hunan Electrical College of Technology, 411101.Xiangtan, PR China, and Changsha Environmental Protection College, Changsha, 410004, People's Republic of China.

References

Abouelregal, A.E. (2018), "Response of thermoelastic microbeams to a periodic external transverse excitation based on MCS theory", *Microsyst. Technol.*, **24**(4), 1925-1933. https://doi.org/10.1007/s00542-017-3589-0.

Abouelregal, A.E. (2020), "Size-dependent thermoelastic initially stressed micro-beam due to a varying temperature in the light of the modified couple stress theory", *Appl. Math. Mech.*, **41**(12), 1805-1820. https://doi.org/10.1007/s10483-020-2676-5.

Abouelregal, A.E. (2021), "Thermoelastic fractional derivative model for exciting viscoelastic microbeam resting on Winkler foundation", *J. Vib. Control*, **27**(17-18), 2123-2135. https://doi.org/10.1177/1077546320956528.

Abouelregal, A.E. (2022), "Modeling and analysis of a thermoviscoelastic rotating micro-scale beam under laser heat models of", *Thin Wall. Struct.*, **174**, 109150. https://doi.org/10.1016/j.tws.2022.109150.

Abouelregal, A.E. (2024), "Effect of non-local modified couple stress theory on the responses of axially moving thermoelastic nano-beams", *ZAMM-Zeitschrift fur Angewandte Mathematik und Mechanik*, **104**(4), 1-22. https://doi.org/10.1002/zamm.202200233.

Abouelregal, A.E. and Tiwari, R. (2022), "The thermoelastic vibration of nano-sized rotating beams with variable thermal properties under axial load via memory-dependent heat conduction", *Meccanica*, **57**(8), 2001-2025. https://doi.org/10.1007/s11012-022-01543-3.

Abouelregal, A.E., Akgoz, B. and Civalek, O. (2022), "Nonlocal thermoelastic vibration of a solid medium subjected to a pulsed heat flux via Caputo-Fabrizio fractional derivative heat conduction", *Appl. Phys. A*, **128**(8), 660. https://doi.org/10.1007/s00339-022-05786-5.

Aghamohammadi, M., Sorokin, V. and Mace, B. (2019), "On the response attainable in nonlinear parametrically excited systems", *Appl. Phys. Lett.*, **115**(15), 154102. https://doi.org/10.1063/1.5120434.

Aghamohammadi, M., Sorokin, V. and Mace, B. (2023), "Nonlinear dynamics of parametrically excited cantilever beams with a tip mass considering nonlinear inertia and Duffing-type nonlinearity", *Nonlin. Dyn.*, **111**(8), 7251-7269. https://doi.org/10.1007/s11071-023-08236-w.

Akbas, S.D., Dastjerdi, S., Akgoez, B. and Civalek, O. (2022), "Dynamic analysis of functionally graded porous microbeams under moving load", *Transp. Porous Media*, **142**(1), 209-227. https://doi.org/10.1007/s11242-021-01686-z.

Al-Furjan, M.S.H., Habibi, M., Jung, D.W., Chen, G.J., Safarpour, M. and Safarpour, H. (2021), "Chaotic

responses and nonlinear dynamics of the graphene nanoplatelets reinforced doubly-curved panel", *Eur. J. Mech. A-Solid.*, **85**, 104091. https://doi.org/10.1016/j.euromechsol.2020.104091.

Alhassan, Y. and Abouelregal, A.E. (2025), "Impact of microscopic interactions and non-Local dynamics on rotating nanobeam structures under external moving loads", *Contin. Mech. Thermodyn.*, **37**(4), 62. https://doi.org/10.1007/s00161-025-01390-z.

Alibakhshi, A., Dastjerdi, S., Akgoz, B. and Civalek, O. (2022), "Parametric vibration of a dielectric elastomer microbeam resonator based on a hyperelastic cosserat continuum model", *Compos. Struct.*, **287**, 115386. https://doi.org/10.1016/j.compstruct.2022.115386.

Alimoradzadeh, M. and Akbas, S.D. (2023), "Nonlinear vibration analysis of carbon nanotube-reinforced composite beams resting on nonlinear viscoelastic foundation", *Geomech. Eng.*, **32**(2), 125-135. https://doi.org/10.12989/gae.2023.32.2.125.

Arvin, H., Arena, A. and Lacarbonara, W. (2020), "Nonlinear vibration analysis of rotating beams undergoing parametric instability: Lagging-axial motion", *Mech. Syst. Signal Pr.*, **144**, 106892. https://doi.org/10.1016/j.ymssp.2020.106892.

Ashraf, M.A., Liu, Z.L., Zhang, D.Q. and Pham, B.T. (2022), "Effects of elastic foundation on the large-amplitude vibration analysis of functionally graded GPL-RC annular sector plates", *Eng. Comput.*, **38**(1), 325-345. https://doi.org/10.1007/s00366-020-01068-x.

Carboni, B., Catarci, S. and Lacarbonara, W. (2022), "Parametric resonances of nonlinear piezoelectric beams exploiting in-plane actuation", *Mech. Syst. Signal Pr.*, **163**, 108119. https://doi.org/10.1016/j.ymssp.2021.108119.

Chai, Y.Y., Li, F.M., Song, Z.G. and Zhang, C.Z. (2020), "Analysis and active control of nonlinear vibration of composite lattice sandwich plates", *Nonlin. Dyn.*, **102**(4), 2179-2203. https://doi.org/10.1007/s11071-020-06059-7.

Chen, W., Wang, L. and Dai, H.L. (2020), "Nonlinear free vibration of hyperelastic beams based on neo-hookean model", *Int. J. Struct. Stab. Dy.*, **20**(1), 2050015. https://doi.org/10.1142/S0219455420500157.

Cheng, Y.H. and She, G.L. (2025a), "Nonlinear transient response of rotating graphene-reinforced metal foam beams with cracks", *Int. J. Struct. Stab. Dyn.*, 2640003. https://doi.org/10.1142/S0219455426400031.

Cheng, Y.H. and She, G.L. (2025b), "Nonlinear combined resonance of graphene platelet-reinforced metal foam beam", *Steel Compos. Struct.*, **56**(3), 265-276. https://doi.org/10.12989/scs.2025.56.3.265.

Cheng, Y.H., She, G.L. and Eltaher, M.A. (2025), "Nonlinear internal resonance of graphene-reinforced metal foam plates with initial geometric imperfection under non-uniform temperature field", *Aerosp. Sci. Technol.*, **165**, 110491. https://doi.org/10.1016/j.ast.2025.110491.

El Khouddar, Y., Adri, A., Outassafte, O., Rifai, S. and Benamar, R. (2021), "An analytical approach to geometrically nonlinear free and forced vibration of piezoelectric functional gradient beams resting on elastic foundations in thermal environments", *Mech. Adv. Mater. Struct.*, **30**(1), 131-143. https://doi.org/10.1080/15376494.2021.2009601.

Fan, Y.H., She, G.L. and Li, C. (2025), "Nonlinear transient response analysis of revolution doubly curved shells", *Arch. Civil Mech. Eng.*, **25**, 145. https://doi.org/10.1007/s43452-025-01187-6.

Foroutan, K. and Ahmadi, H. (2022), "Nonlinear parametric vibration of imperfect SSMFG cylindrical shells in thermal environment including internal and subharmonic resonances", *Mech. Adv. Mater. Struct.*, **29**(24), 3499-3522. https://doi.org/10.1080/15376494.2021.1904526.

Garg, A. and Dwivedy, S.K. (2020), "Dynamic analysis of piezoelectric energy harvester under combination parametric and internal resonance: a theoretical and experimental study", *Nonlin. Dyn.*, **101**(4), 2107-2129. https://doi.org/10.1007/s11071-020-05931-w.

Gu, X.J., Zhang, W. and Zhang, Y.F. (2021), "Nonlinear vibrations of rotating pretwisted composite blade reinforced by functionally graded graphene platelets under combined aerodynamic load and airflow in tip clearance", *Nonlin. Dyn.*, **105**(2), 1503-1532. https://doi.org/10.1007/s11071-021-06681-z.

Hamed, Y.S. and Alkhathami, H.K. (2021), "On the nonlinear vibrations and stability analysis of a plate-cavity system with a nonlinear restoring force", *IEEE Access*, **9**, 20423-20439. https://doi.org/10.1109/ACCESS.2021.3054517.

Hasan, A.M.Z. and Rahman, M.S. (2022), "Multi-level residue harmonic balance method for nonlinear vibration of the beam", *J. Low Freq. Noise Vib. Act. Control*, **41**(1), 278-291. https://doi.org/10.1177/14613484211038403.

Hosseini, S.A.H., Rahmani, O., Refaeinejad, V., Golmohammadi, H. and Montazeripour, M. (2023), "Free vibration of deep and shallow curved FG nanobeam based on nonlocal elasticity", *Adv. Aircraft Spacecraft Sci.*, **10**, 51-65. https://doi.org/10.12989/aas.2023.10.1.051.

Hu, Y.D., Li, Z., Du, G.J. and Wang, Y.N. (2018), "Magneto-elastic combination resonance of rotating circular plate with varying speed under alternating load", *Int. J. Struct. Stab. Dyn.*, **18**(3), 1850032. https://doi.org/10.1142/S0219455418500323.

Hu, Y.D., Rong, Y.T. and Li, J. (2018), "Primary parametric resonance of an axially accelerating beam subjected to static loads", *J. Theor. Appl. Mech.*, **56**(3), 815-828. https://doi.org/10.15632/jtam-pl.56.3.815.

Jahangiri, R., Rezaee, M. and Manafi, H. (2022), "Nonlinear and chaotic vibrations of FG double curved sandwich shallow shells resting on visco-elastic nonlinear Hetenyi foundation under combined resonances", *Compos. Struct.*, **295**, 115721. https://doi.org/10.1016/j.compstruct.2022.115721.

Le, C.I. and Nguyen, D.K. (2023), "Nonlinear vibration of three-phase bidirectional functionally graded sandwich beams with influence of homogenization scheme and partial foundation support", *Compos. Struct.*, **307**, 116649. https://doi.org/10.1016/j.compstruct.2022.116649.

Li, X. (2021), "Parametric resonances of rotating composite laminated nonlinear cylindrical shells under periodic axial loads and hygrothermal environment", *Compos. Struct.*, **255**, 112887. https://doi.org/10.1016/j.compstruct.2020.112887.

Li, X.Q., Song, M.T., Yang, J. and Kitipornchai, S. (2019), "Primary and secondary resonances of functionally graded graphene platelet-reinforced nanocomposite beams", *Nonlin. Dyn.*, **95**(3), 1807-1826. https://doi.org/10.1007/s11071-018-4660-9.

Li, Y.P. and She, G.L. (2025), "Nonlinear dynamic response of graphene platelets reinforced cylindrical shells under moving loads considering initial geometric imperfection", *Eng. Struct.*, **323**(A), 119241. https://doi.org/10.1016/j.engstruct.2024.119241.

Li, Z., Hu, Y.D. and Li, J. (2017), "Magnetoelastic principal parametric resonance of a rotating electroconductive circular plate", *Shock Vib.*, **2017**, 5196847. https://doi.org/10.1155/2017/5196847.

Li. H.Y., Zhang, S.M., Li, J. and Wang, X.B. (2020), "Parametric resonance of axially accelerating unidirectional plates partially immersed in fluid", *J. Comput. Nonlin. Dyn.*, **15**(10), 101002. https://doi.org/10.1115/1.4047483.

Liu, T., Zhang, W. and Wang, J.F. (2017), "Nonlinear dynamics of composite laminated circular cylindrical shell clamped along a generatrix and with membranes at both ends", *Nonlin. Dyn.*, **90**(2), 1393-1417. https://doi.org/10.1007/s11071-017-3734-4.

Ma, Z.S., She, G.L. and Li, C. (2025), "Nonlinear thermal flutter analysis of graphene platelets reinforced metal foam arbitrary quadrilateral plates", *Arch. Civil Mech. Eng.*, **25**, 203. https://doi.org/10.1007/s43452-025-01262-y.

Mbong, T.L.M.D., Siewe, M.S. and Tchawoua, C. (2018), "Controllable parametric excitation effect on linear and nonlinear vibrational resonances in the dynamics of a buckled beam", *Commun. Nonlin. Sci.*, **54**, 377-388. https://doi.org/10.1016/j.cnsns.2017.06.019.

Mirjavadi, S.S., Forsat, M., Hamouda, A. and Barati, M.R. (2019), "Dynamic response of functionally graded graphene nanoplatelet reinforced shells with porosity distributions under transverse dynamic loads", *Mater. Res. Expr.*, **6**(7), 075045. https://doi.org/10.1088/2053-1591/ab1552.

Mohamed, N., Mohamed, S.A. and Eltaher, M.A. (2024), "Exact solutions of vibration and postbuckling response of curved beam rested on nonlinear viscoelastic foundations", *Adv. Aircraft Spacecraft Sci.*, **11**, 55-81. https://doi.org/10.12989/aas.2024.11.1.055.

Rincon-Casado, A., Gonzalez-Carbajal, J., Garcia-Vallejo, D. and Dominguez, J. (2021), "Analytical and numerical study of the influence of different support types in the nonlinear vibrations of beams", *Eur. J. Mech. A-Solid.*, **85**, 104113. https://doi.org/10.1016/j.euromechsol.2020.104113.

Sahoo, B. (2020), "Nonlinear dynamics of a viscoelastic beam traveling with pulsating speed, variable axial

tension under two-frequency parametric excitations and internal resonance", *Nonlin. Dyn*., **99**(2), 945-979. https://doi.org/10.1007/s11071-019-05264-3.

Sahoo, B. (2022), "Multi-scale analysis of a moving beam under parametric and auto-parametric resonances", *J. Brazil. Soc. Mech. Sci*., **44**(1), 20. https://doi.org/10.1007/s40430-021-03303-y.

Sahoo, B., Panda, L.N. and Pohit, G. (2017), "Stability, bifurcation and chaos of a traveling viscoelastic beam tuned to 3: 1 internal resonance and subjected to parametric excitation", *Int. J. Bifurcat. Chaos*, **27**(2), 1750017. https://doi.org/10.1142/S0218127417500171.

Sahoo, P.K. and Chatterjee, S. (2021), "High-frequency vibrational control of principal parametric resonance of a nonlinear cantilever beam: Theory and experiment", *J. Sound. Vib*., **505**, 116138. https://doi.org/10.1016/j.jsv.2021.116138.

Shao, Y.F. and Ding, H. (2023), "Evaluation of gravity effects on the vibration of fluid-conveying pipes", *Int. J. Mech. Sci*., **248**, 108230. https://doi.org/10.1016/j.ijmecsci.2023.108230.

She, G.L., Gan, L.L. and Xu, J.Q. (2025), "Nonlinear snap-buckling of graphene platelet reinforced metal foams doubly curved shells with geometric imperfection", *Geomech. Eng.*, **40**(3), 183-191. https://doi.org/10.12989/gae.2025.40.3.183.

Sheng, G.G. and Wang, X. (2018), "Nonlinear vibration of FG beams subjected to parametric and external excitations", *Eur. J. Mech. A-Solid*., **71**, 224-234. https://doi.org/10.1016/j.euromechsol.2018.04.003.

Teng, M.W. and Wang, Y.Q. (2021), "Nonlinear forced vibration of simply supported functionally graded porous nanocomposite thin plates reinforced with graphene platelets", *Thin. Wall. Struct*., **164**, 107799. https://doi.org/10.1016/j.tws.2021.107799.

Wang, L., Yang, J. and Li, Y.H. (2021), "Nonlinear vibration of a deploying laminated Rayleigh beam with a spinning motion in hygrothermal environment", *Eng. Comput*., **37**(4), 3825-3841. https://doi.org/10.1007/s00366-020-01035-6.

Wang, T.Q., Wang, R.H. and Ma, N.J. (2019), "Nonlinear vibration of a stiffened plate considering the existence of initial stresses", *KSCE J. Civil Eng*., **23**(5), 2303-2312. https://doi.org/10.1007/s12205-019-1387-1.

Wang, W.Q., Ye, C. and Zu, J.W. (2019), "Nonlinear vibration of metal foam cylindrical shells reinforced with graphene platelets", *Aerosp. Sci. Technol*., **85**, 359-370. https://doi.org/10.1016/j.ast.2018.12.022.

Wang, Y., Jing, X., Dai, H. and Li, F. (2019b), "Subharmonics and ultra-subharmonics of a bio-inspired nonlinear isolation", *Int. J. Mech. Sci*., **152**, 167-184. https://doi.org/10.1016/j.ijmecsci.2018.12.054.

Wang, Y., Li, F. and Shu, H. (2019a), "Nonlocal nonlinear chaotic and homoclinic analysis of double layered forced viscoelastic nanoplates", *Mech. Syst. Signal Pr.*, **122**, 537-554. https://doi.org/10.1016/j.ymssp.2018.12.041.

Wang, Y., Liu, J., Li, J., Jing, X. and Wiercigroch, M. (2025), "Intrinsic mechanisms of vibrational mode jumping in sandwich panels", *J. Sound Vib.*, **618**(Part B), 119247. https://doi.org/10.1016/j.jsv.2025.119247.

Wang, Y.W. and Zhang, W. (2022), "On the thermal buckling and postbuckling responses of temperature-dependent graphene platelets reinforced porous nanocomposite beams", *Compos. Struct*., **296**, 115880. https://doi.org/10.1016/j.compstruct.2022.115880.

Wang, Y.W., Xie, K., Fu, T.R. and Shi, C.L. (2019), "Vibration response of a functionally graded graphene nanoplatelet reinforced composite beam under two successive moving masses", *Compos. Struct*., **209**, 928-939. https://doi.org/10.1016/j.compstruct.2018.11.014.

Xie, K., Wang, Y.W. and Fu, T.R. (2020), "Nonlinear vibration analysis of third-order shear deformable functionally graded beams by a new method based on direct numerical integration technique", *Int. J. Mech. Mater. Des*., **16**(4), 839-855. https://doi.org/10.1007/s10999-020-09493-y.

Xiong, X., Wang, Y., Li, J. and Li, F. (2023), "Internal resonance analysis of bio-inspired X-shaped structure with nonlinear vibration absorber", *Mech. Syst. Signal Pr.*, **185**, 109809. https://doi.org/10.1016/j.ymssp.2022.109809.

Xu, H., Wang, Y.Q. and Zhang, Y.F. (2021), "Free vibration of functionally graded graphene platelet-reinforced porous beams with spinning movement via differential transformation method", *Arch. Appl. Mech*., **91**(12), 4817-4834. https://doi.org/10.1007/s00419-021-02036-7.

Xu, J.Q., Li, Y.P. and She, G.L. (2025), "Nonlinear low-velocity impact response of GPLRMF doubly curved shells in thermal environment", *Comput. Concrete*, **35**(3), 219-229. https://doi.org/10.12989/cac.2025.35.3.219.

Yang, C.M., Jin, G.Y., Zhang, J.H., Ye, T.G. and Liu, Z.G. (2021), "A unified Fourier spectral method for nonlinear free vibration analysis of the laminated composite and sandwich beams with arbitrary restrained ends", *J. Brazil. Soc. Mech. Sci. Eng*., **43**(9), 432. https://doi.org/10.1007/s40430-021-03150-x.

Yang, F.L., Wang, Y.Q. and Liu, Y.F. (2022), "Low-velocity impact response of axially moving functionally graded graphene platelet reinforced metal foam plates", *Aerosp. Sci. Technol*., **123**, 107496. https://doi.org/10.1016/j.ast.2022.107496.

Yang, J. and Chen, Y. (2008), "Free vibration and buckling analyses of functionally graded beams with edge cracks", *Compos. Struct*., **83**(1), 48-60. https://doi.org/10.1016/j.compstruct.2007.03.006.

Zhang, Y.F., Zhang, W. and Yao, Z.G. (2018), "Analysis on nonlinear vibrations near internal resonances of a composite laminated piezoelectric rectangular plate", *Eng. Struct*., **173**, 89-106. https://doi.org/10.1016/j.engstruct.2018.04.100.

Zhang, Z., Gao, Z.T., Fang, B. and Zhang, Y.W. (2022), "Vibration suppression of a geometrically nonlinear beam with boundary inertial nonlinear energy sinks", *Nonlin. Dyn*., **109**(3), 1259-1275. https://doi.org/10.1007/s11071-022-07490-8.

Zhao, B. and She, G.L. (2025), "Vibration analysis of graphene reinforced metal foam coupled plates under arbitrary boundary and coupled conditions", *Eng. Struct.*, **343**, 121143. https://doi.org/10.1016/j.engstruct.2025.121143.

Zhao, Y.H., Du, J.T., Chen, Y.L. and Liu, Y. (2023), "Nonlinear dynamic behavior of a generally restrained pre-pressure beam with a partial non-uniform foundation of nonlinear stiffness", *Int. J. Struct. Stab. Dyn*., **23**(03), 2350028. https://doi.org/10.1142/S0219455423500281.

Zhou, Y.X., Zhang, Y.M. and Yao, G. (2021), "Nonlinear forced vibration analysis of a rotating three-dimensional tapered cantilever beam", *J. Vib. Control*, **27**(15-16), 1879-1892. https://doi.org/10.1177/1077546320949716.

Zhu, B., Dong, Y.H. and Li, Y.H. (2018), "Nonlinear dynamics of a viscoelastic sandwich beam with parametric excitations and internal resonance", *Nonlin. Dyn*., **94**(4), 2575-2612. https://doi.org/10.1007/s11071-018-4511-8.

Zhu, B., Xu, Q., Li, M. and Li, Y.H. (2020), "Nonlinear free and forced vibrations of porous functionally graded pipes conveying fluid and resting on nonlinear elastic foundation", *Compos. Struct*., **252**, 112672. https://doi.org/10.1016/j.compstruct.2020.112672.

CC